Interactions Between Isolated Pea Globulins and Purified Egg White Proteins in Solution

Jian Kuang, Pascaline Hamon, Florence Rousseau, Eliane Cases, Said
Bouhallab, Rémi Saurel, Valerie Lechevalier

RESEARCH

Interactions Between Isolated Pea Globulins and Purified Egg White Proteins in Solution

Jian Kuang[1,2] · Pascaline Hamon[2] · Florence Rousseau[2] · Eliane Cases[1] · Saïd Bouhallab[2] · Rémi Saurel[1] · Valerie Lechevalier[2]

© The Author(s), under exclusive licence to Springer Science+Business Media, LLC, part of Springer Nature 2023

Abstract

In the present work, the interactions and associations between low denatured pea globulins (PPI) and purified main egg white proteins (ovalbumin (OVA), ovotransferrin (OVT), and lysozyme (LYS)) were studied at pH 7.5 and 9.0 by using isothermal titration calorimetry (ITC), dynamic light scattering (DLS), laser granulometry and confocal laser scanning microscopy (CLSM). From ITC, we detected strong exothermic interactions between PPI and LYS at both pHs, which led to aggregation. At these pH values, the net positive charge of lysozyme favored electrostatic interactions with negative charges of pea proteins, and oligomers were formed during titration experiments. Furthermore, DLS, laser granulometry, and CLSM data showed that the particle size of the mixture increased with increasing LYS to PPI molar ratio (from 0.8 to 20). Large irregular aggregates up to 20–25 μm were formed at high molar ratios and no complex coacervate was observed. No or very weak interactions were detected between OVT or OVA and PPI whatever the pH. These results suggest the role of electrostatic interactions between LYS and PPI when considering protein mixtures.

Keywords Interactions · Pea protein isolate · Lysozyme · ITC · DLS · Confocal microscopy

Introduction

With the increase in world population and food transition in emerging countries, the demand for protein is expected to double by 2050 [1]. The demand for animal proteins increases in emerging countries, which is a ticking time bomb in terms of sustainability and food security, as noted by various United Nations assessments [2, 3]. However, raw animal materials like milk, eggs, meat, and seafood continue to be the most important sources of protein recently employed by food companies, followed by plant sources like legumes and nuts [4]. Meanwhile, animal protein production is connected with high greenhouse gas emissions and increased land requirements, whereas plant proteins have a lower economic cost and lower ecological footprint [4, 5]. Legumes proteins, on the other hand, are produced for

animal feed yet having physicochemical features that make them valuable for human consumption [6]. Furthermore, excessive intake of animal proteins can have a severe influence on human health, including the development of illnesses such as obesity, cardiovascular disease, neurological disorders, allergies, and so on [7]. As a result, the partial substitution of animal protein with plant protein is gaining popularity in designed goods [8–11]. They are frequently sold as "healthier" and sustainable new foods as "substitutes" for traditional animal-derived food items [12]. However, studies dealing with partial substitution of animal protein by plant protein mainly deals with milk or meat proteins as animal sources. Despite they are the most sustainable animal proteins, there is thus currently a lack of research on egg proteins as an animal source of protein blended with plant protein.

Egg is well-known for its high nutritional content, great digestibility, and full essential amino acid supply. Egg white, especially is widely used for its foaming and gelling properties. Proteins indeed account for more than 90% of the dry substance in egg white, giving it its single functional properties. It is a good candidate for mixing with plant proteins, especially because its basic pH (from 7.5 just after laying to

✉ Valerie Lechevalier
   valerie.lechevalier@agrocampus-ouest.fr

1   Université Bourgogne Franche-Comté, L'Institut Agro Dijon, PAM UMR A 02.102, 21000 Dijon, France

2   UMR STLO, INRAE, L'Institut Agro Rennes-Angers, 65 rue de Saint Brieuc, 35042 Rennes Cedex, France

9.5 a few days later) may help their solubilization. Egg white contains more than 40 different proteins. Ovalbumin (OVA) is the major one and represents about 54% of the total egg white proteins, while ovotransferrin (OVT) and lysozyme (LYS) constitute about 12% and 3.4%, respectively [13, 14]. OVA is a peptide chain containing 385 amino acid residues and its isoelectric point is 4.5. It has a molecular weight of 44.5 kDa and contains four thiols and one disulfide bond. OVT is a glycosylated peptide chain of 686 amino acids. Its molecular weight is 77.7 kDa and its isoelectric point is 6.1. OVT has 15 disulfide bonds and about 55% reactive residues. LYS is a relatively small secretory glycoprotein, consisting of 129 amino acids linked by four disulfide bonds. It is a 14.4 kDa protein with an isoelectric point of 10.7 [15–17].

A few works were dedicated to the study of gelation and thermal aggregation of egg white protein mixed with soy protein [18, 19], or cold gelation of egg and hempseed proteins [20]. Complex formation through electrostatic interactions and hydrogen bonds between lysozyme (LYS) and soy protein isolates was highlighted by Zheng et al. [21]. However, no study was found on mixtures of egg white proteins and pea proteins. Yet, recently, there has been a lot of attention in pea proteins (Pisum Sativum L), which have a lot of promises in the food supply because of their high yields and low pricing [22, 23]. Peas are one of the world's most frequently farmed and consumed legumes, namely in Canada, France, China, Russia, and the United States [6, 24]. Pea proteins have quite comparable functional qualities as soy proteins however it is non-allergenic [25]. This protein source is thought to be a viable alternative to animal and soy proteins [24, 26]. However, there are some limits for pea proteins to be used as an ingredient, primarily due to a lack of understanding of their structure and functional features [26, 27]. Protein accounts for 20–30% of pea seed, which mainly consists in globulins and albumins. Globulins, known as salt-soluble proteins, represent around 50–60% of total pea proteins while the water-soluble albumins accounted for 15–25% [28]. Meanwhile, legumin (11 S) and vicilin/convicilin (7 S) constitute pea globulins. Legumin is a hexameric homo-oligomer with a molecular weight (Mw) of 360–400 kDa. Each subunit is around 60 kDa which consists in an acidic (~40 kDa) and a basic polypeptide (~20 kDa) linked by a disulfide bond. The acidic chain also has one free thiol [29, 30]. Vicilin is a trimeric protein with a molecular weight of around 150 kDa, where the main vicilin subunit (~50 kDa) can undergo in vivo proteolysis at two potential cleavage sites. The vicilin-associated protein, convicilin, is a 210–290 kDa protein, consisting of subunits (~71 kDa) associated in trimeric or tetrameric form [30].

Few studies were carried out on the interactions between pea protein isolate and animal protein. However, Mession et al. [31] investigated the aggregation of proteins after heat treatment of a mixed system constituted of casein micelles and pea globulins separated into vicilin and legumin. In admixture, casein micelles were not engaged in pea protein aggregation, even though heat-induced pea protein interactions were changed compared to pure pea protein systems. More recently, Kristensen et al. [32–34] studied interactions between pea and whey protein isolates. Under neutral or alkaline pH, a simple mixing of these proteins, increased their solubility, emulsifying and foaming abilities compared to separated protein. The co-aggregates formed by the heating of the mixture of these proteins implied electrostatic interactions and disulfide bonds, especially between pea legumin and β-lactoglobulin [35, 36].

Although more and more researches focus on the mixtures of plant protein and animal proteins, they mainly concern soy and dairy proteins. The mixture of egg white proteins as a sustainable animal protein source and pea proteins as a promising non-allergenic plant protein source has not been studied yet.

To better understand the behavior of these two protein sources in association in food systems, this study proposes a first approach to investigate the interactions between pea globulins and purified egg white proteins in aqueous mixtures at neutral and alkaline pH (pH 7.5 and 9.0), close to that of egg white. The potential interaction of whole pea globulins with purified LYS, OVA, or OVT was firstly examined by isothermal titration calorimetry (ITC) and ζ-potential measurements. The detected attractive interactions between LYS and pea globulins were further explored at different pH via characterization of formed structures by dynamic light scattering (DLS), laser granulometry, and confocal laser scanning microscopy (CLSM).

Materials and Methods

Protein Extraction

Pea globulins were extracted from smooth yellow pea flour (P. sativum L.), supplied by Cosucra (Lestrem, France). Isoelectric-precipitation technique was used to prepare pea protein isolate (PPI), containing mainly globulins, based on the method of Chihi et al. [36] with some modifications. Pea flour was mixed with distilled water at 100 g/L, and the pH was adjusted to pH 8 with 1 M NaOH every two hours and stirred overnight at 4℃. After adjusting the pH, insoluble materials were removed by centrifugation (10 000 g, 30 min, 25℃) and the recovered solution was adjusted to pH 4.8 by using 0.5 M HCl. After acidification, the precipitated proteins were recovered by centrifugation (10 000 g, 25 min, 4℃). Afterward, the pellets were dissolved in 5 L 0.1 M phosphate buffer at pH 8 overnight at 4℃ for complete dissolution. The protein suspension was obtained by centrifugation (10 000 g, 20 min, 20℃) and then concentrated 5 times by ultrafiltration (from 5 L to 800–900 mL) and desalted by diafiltration against 10 L 5 mM ammonium buffer pH 7.2 and 0.05% sodium azide on an 1115 cm² Kvick lab Cassette

(UFELA0010010ST, GE Healthcare, Amersham Biosciences, Uppsala, Sweden) with a molecular weight cut-off of 10 kDa. Protein powder (89% based on dry basis) as PPI was obtained after freeze-drying. Differential scanning calorimetry analysis indicated the recovery of low denaturized PPI after the extraction procedure (data not shown).

OVA was extracted from fresh eggs from the local market according to Croguennec et al. [37]. Egg white recovered from 12 eggs were diluted with 1:2 (v/v) volumes of distilled water, then the pH was adjusted to pH 6.0 with 1 M HCl to precipitate ovomucin. Subsequently, the solution was stirred at 4℃ overnight. Then the supernatant was recovered after centrifugation (10 000 *g*, 4℃, 30 min) and adjusted to pH 8.4 with 5 M NaOH. After centrifugation (10 000 *g*, 25℃, 25 min), the supernatant was filtered with a plastic strainer and injected to an anion exchange chromatography Q-Sepharose Fast flow column (Pharmacia Biotech AB, Saclay, France) to separate the OVA from the other egg white proteins. The OVA (96% protein content) powder was obtained after freeze-drying. OVT (94% protein content) and LYS (95% protein content) were supplied from EUROVO (Annezin-les-Béthunes, France and Occhiobello, Italy, respectively). All other reagents and chemicals purchased from Sigma-Aldrich (St-Quentin Fallavier, France) were of analytical grade.

Protein Content

The protein content was measured according to Kjeldahl AOAC International method 920.87. [38] with nitrogen-to-protein conversion factors of 5.44 for pea proteins [39] and 6.32 for egg proteins [40].

Protein Stock Solutions

Stock solutions of PPI (0.008 mM, considering an average molecular weight of 236 kDa as explained in Section Isothermal titration calorimetry (ITC)), LYS (0.92 mM), OVA (1.65 mM), and OVT (0.66 mM) were prepared by solubilizing the protein powders either in 10 mM HEPES at pH 7.5 or in 10 mM TRIS buffer at pH 7.5 or pH 9.0 and stirred mechanically at 400 rpm over 3 h at room temperature to ensure complete hydration of the protein powders. The insoluble protein part was estimated as negligible. The pH of the protein suspensions was then adjusted by 0.1 M HCl or NaOH before each test.

Isothermal Titration Calorimetry (ITC)

ITC experiments were carried out using an VP-ITC microcalorimeter (Microcal, Northampton, MA) with a standard volume of 1.425 mL at 25℃. Stock solutions were filtered through 0.2 μm filters and degassed under vacuum to guarantee no bubbles inside the solutions. The solutions of PPI, egg white proteins (LYS, OVA, OVT), and buffer were placed in the reaction cell, syringe, and reference cell respectively. A total number of 29 injections of egg white protein stock solutions (10 μL of each) were performed after the calorimeter finalized the primary equilibration, with 200 s interval between the injections, leaving 60 s at the beginning of the experiment before the first injection. The stirring rate was set at 300 rpm. Data resulting from the subtraction of reference values (dilution heat) from the sample values were analyzed by Micro ORIGIN version 7.0 (Microcal, Northampton, MA). Control experiments were performed in each case by titrating the egg white protein into the buffer and were subtracted from raw data to determine corrected enthalpy changes. Each ITC data were collected by at least two independent measurements and reproducible data was employed.

To analyze ITC results in terms of LYS/PPI molar ratio variation, the mean molecular weight of globulins in PPI (Mw PPI) was approximated by the following equation:

$$Mw\ PPI = (Mw\ PPI - 11\ S).(11\ S - to - (7\ S + 11\ S)\ ratio)$$
$$+ (Mw\ PPI - 7\ S).(7\ S - to - (7\ S + 11\ S)\ ratio) \quad (1)$$

with Mw PPI-11 S = 360 kDa, Mw PPI-7 S = 150 kDa, and 11 S-to-(7 S + 11 S) ratio = 0.41 and 7 S-to-(7 S + 11 S) ratio = 0.59; the two last ratios were deduced from enthalpy area deconvolution from Differential Scanning Calorimetry spectra showing two characteristic peaks considering 7 and 11 S pea proteins had the same denaturation enthalpy (data not shown).
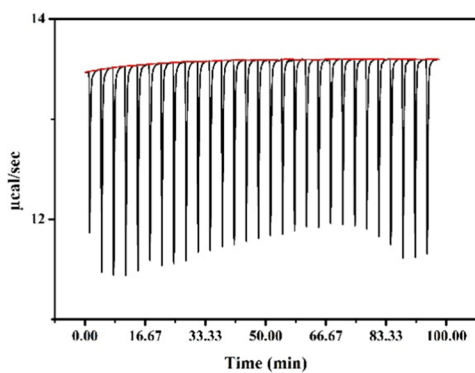
The Mw PPI value was thus estimated at 236 kDa.

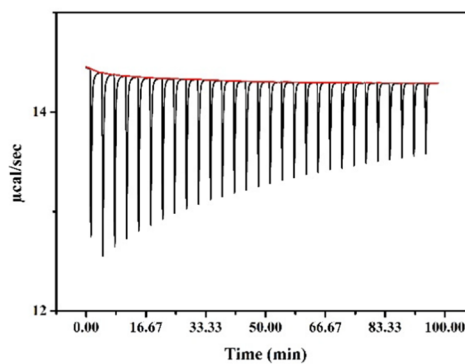## Dynamic Light Scattering (DLS) and Laser Granulometry

The size distribution of PPI and LYS was determined by DLS (Nanosizer, Malvern Instruments, UK). PPI and LYS stock solutions were first diluted 5 times in Tris-HCl buffer at pH 7.5 or 9.0, before measurement. PPI (0.008 mM) and LYS (0.92 mM) stock solutions were then mixed at 10 different LYS/PPI molar ratios (3.2, 4.8, 6.4, 8.0, 9.6, 11.2, 12.8, 14.4, 21.0, 23.2 and 5.2, 8.7, 12.2, 14.0, 15.7, 17.5, 19.2, 20.9, 23.6, 25.3 at pH 7.5 and 9.0, respectively) corresponding to 10 ratios distributed all along the ITC titration curve. The size distribution of the particles in the different molar ratio LYS-PPI mixtures was determined by laser granulometry (Mastersizer 2000, Malvern Instruments, UK).
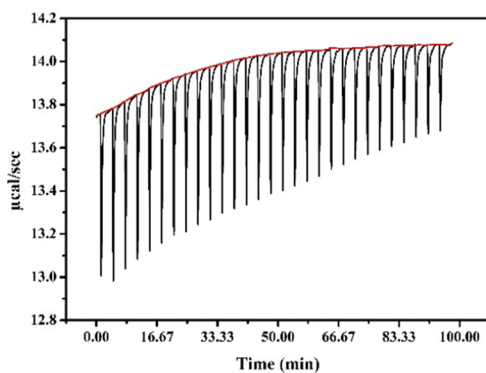
ζ-Potential

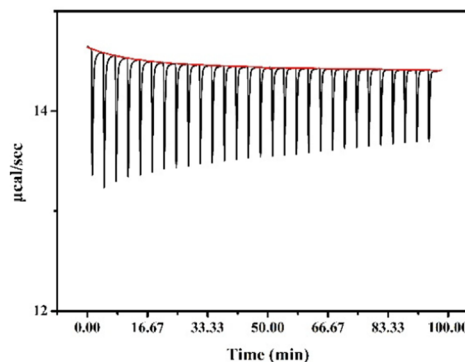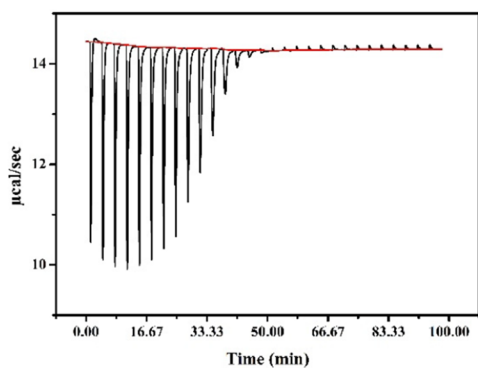The ζ-potential of PPI (0.008 mM), LYS (0.92 mM), and their mixtures prepared in TRIS buffer at pH 7.5
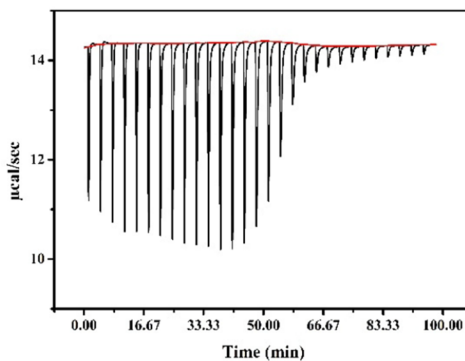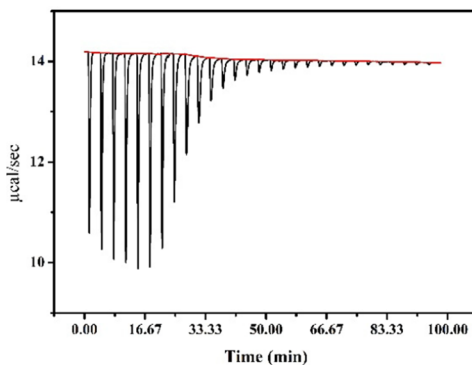
(a1)

(a2)

(b1)

(b2)

(c1)

(c2)

(d)

◄ **Fig. 1** Thermograms for the titration of PPI (0.008 mM) with OVA (1.65 mM) in HEPES buffer pH 7.5 (**a1**) and in Tris-HCl buffer pH 9.0 (**a2**), with OVT (0.66 mM) in HEPES buffer pH 7.5 (**b1**) and in Tris-HCl buffer pH 9.0 (**b2**), with LYS (0.92 mM) in HEPES buffer pH 7.5 (**c1**) and in Tris-HCl buffer pH 9.0 (**c2**), with LYS (0. 92 mM) in Tris buffer pH 7.5 (**d**). All the titration experiments were performed at 25 °C

and 9.0 at the 10 LYS/PPI molar ratios described before was determined in the pH range of 2–12 using a Malvern Zetasizer Nano ZS (Nanosizer, Malvern Instruments, UK). 0.1-1 M HCl or NaOH was used to adjust pH from 2 to 12. The ζ-potential was measured at 25°C using a laser Doppler velocimetry and phase analysis light scattering (M3-PALS0) using disposable electrophoretic mobility cells (DTS1070). The equilibration time was set at 120 s, and at least 11 runs were performed for each measurement. The measurements were repeated three times for each sample (PPI, LYS, and LYS-PPI mixtures at pH 7.5 and 9.0).

Confocal Laser Scanning Microscopy (CLSM)

Protein particle formation for LYS-PPI mixtures in TRIS buffer at pH 7.5 at 20 °C was observed by confocal laser scanning microscopy (CLSM) using a ZEISS LSM 880 inverted confocal microscope (Carl Zeiss AG, Oberkochen, Germany) using the methods previously developed by Halabi et al. [41] and Somaratne et al. [42]. Images were observed inside the channel slide system using the high-resolution mode of the confocal microscope equipped with the Airyscan detection unit and a Plan Apochromat 63x with a high numerical aperture (NA = 1.40) oil objective. Samples (200 μL) were gently mixed with Fast Green aqueous solution (1% w/v; 6 μL) and the mixture was kept in dark at 20 °C for at least 10 min. 20 μL of the mixture was deposited on a glass slide in a spacer and a coverslip was placed on top of all samples. Fast green was excited using a He–Ne laser system at a wavelength of 633 nm at a 1.72 μs pixel dwell scanning rate and detected using a PMT between 635 and 735 nm. Images were processed using confocal acquisition software Zen Black 2.1 (Version 13.0.0.0) to process the acquired datasets using the 2D mode at default setting of the Airyscan processing function.

Statistical Analysis

Values were expressed as means ± standard deviations of triplicate determinations. The significant difference was determined at the $P < 0.05$ level for the ONE-WAY Analysis of variance test by using STATISTICA 12 (64 BIT) software.

Results and Discussions

Electrostatic Interactions Between LYS and PPI

The ITC method was used to provide a detailed thermodynamic description and a better understanding of the mechanism of interactions of PPI and egg white proteins in solution. The ITC profiles for PPI with OVA (as acidic protein), OVT (as neutral protein), and LYS (as basic protein) were measured. The heat flow versus time profiles resulting from the titration of the PPI with the three egg proteins at various conditions are shown in Fig. 1.
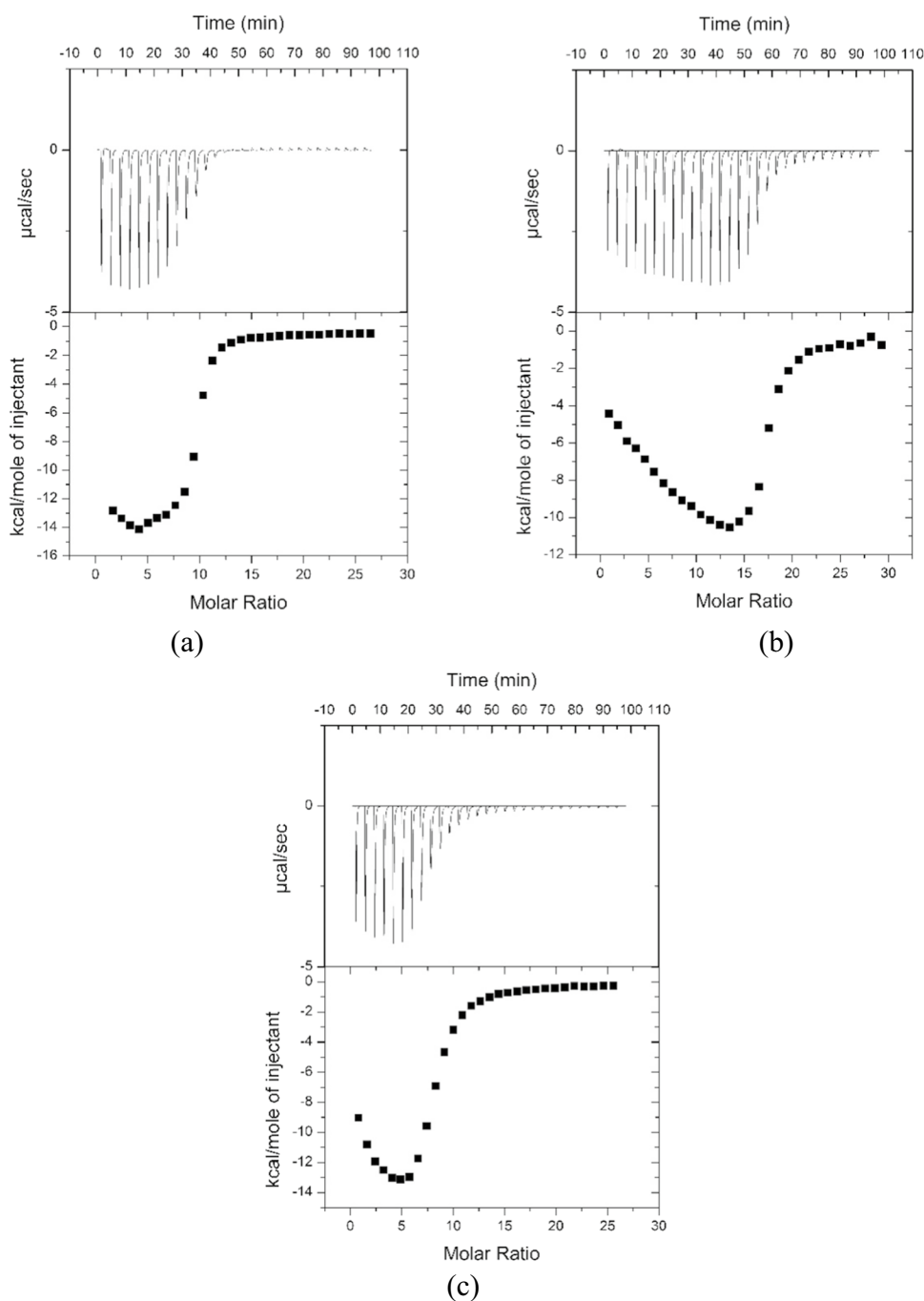
Whatever the egg protein studied, the ITC signal exhibited an exothermic profile. However, the signal intensity depended on the protein injected and the pH value (Fig. 1). Weak interactions were observed between OVA or OVT and PPI at both pHs (7.5 and pH 9.0) (Fig. 1a1, a2, b1, b2). The observed interactions in these mixed systems exhibited a saturating behavior but the signals were too weak to allow access to the thermodynamic parameters. These results suggested that when mixed with PPI, OVA or OVT co-existed in solution without co-aggregation or complexation at neutral to basic pH values and low ionic strength. In contrast, when LYS was injected on PPI, a large exothermic signal was obtained at pH 7.5 but also at pH 9.0 (Fig. 1c1, c2). Meanwhile, to be consistent with the same buffer at both pH, and to avoid the potential buffer/protein interaction already reported by Rabiller-Baudry & Chaufer [43], LYS in TRIS-HCl buffer at pH 7.5 was kept for further analyses.

The strong interaction between LYS and PPI was further explored. Figure 2 shows the ITC profiles and corresponding binding isotherms of the injection of LYS into PPI solution at pH 7.5 and 9.0. The isotherms resulting from titrating PPI with LYS exhibited a visually obvious biphasic profile. The initially integrated heats of injection show a trend toward increasingly negative enthalpy, while later data trend positively until saturation was reached.

The area under each peak represented the heat exchange within the ITC cell after each injection, after subtraction of the heat of dilution of LYS into the buffer solution. While the overall ITC profiles were similar at both pH values, the enthalpy of the interaction was higher at pH 7.5 than at pH 9.0. The observed difference does not seem to be linked to the buffer nature as observed in other protein systems [44]. Indeed, the same ITC signal was recovered at pH 7.5 when HEPES-buffer was substituted by Tris-HCl (Fig. 2a, c).

At both pHs studied, a strong biphasic exothermic signal was obtained, underlying at least two distinct events. During the first phase, the height of the exothermic peaks continuously increased with the addition of LYS until a critical value of LYS/PPI molar ratio beyond which the trend was reversed; further addition of LYS decreased the exothermic intensity of

Fig. 2 Thermograms (top panels) and binding isotherms (bottom panels) for the titration of PPI (0.008 mM) with LYS (0.92 mM) in HEPES buffer pH 7.5 (**a**), in Tris-HCl buffer pH 9.0 (**b**), and in Tris-HCl buffer pH 7.5 (**c**). All the titration experiments were performed at 25 °C

the signal (phase 2) until saturation. By comparing the general appearance of the two signals, two major linked differences could be noticed: (i) the slope of the two phases was steeper at pH 7.5 than at pH 9.0; (ii) the critical inversion LYS/PPI molar ratio shifted to higher-value at pH 9.0, i.e., around 13 against 5 at pH 7.5. Similar biphasic ITC profiles were reported for other heteroprotein systems involving LYS such as LYS/bovine lactalbumin at 45 °C [45] and LYS/conglycinin [46]. Such results were explained by ionic complexation between oppositely charged polymers forming supramolecular structures.

The shift of the molar ratio can be explained by the change of the negative-positive charge balance at the surface of the proteins, in particular LYS given its high isoelectric point (Ip). At pH 9.0, a value approaching its Ip (i.e., 10.7), the LYS is less positively charged than at pH 7.5. Consequently, more LYS molecules are required to neutralize the actual number of negative charges on one PPI molecule, which do not vary significantly from pH 7.5 to pH 9.0. Charge compensation is the main parameter driving electrostatic complexation between oppositely charged proteins [47].

The explanation of what happens during the two phases was not simple since each thermodynamic signal could be the result of the contribution of several phenomena: classical interaction, protein conformational change, release of water, protons, and other ions, complexation, reorganizations, aggregation, etc. [48]. The measured signal, therefore, comes from endothermic and exothermic reactions whose final absolute value is the result of the dominant energy.

To go further in the exploration of the thermodynamic changes occurring during titration, we tried to fit the binding isotherms using different binding models offered by Microcal Origin software. The 'two sets of sites' model seems to better match with the experimental titration profiles (data not shown). However, as already pointed out by other authors relating to other macromolecular systems [49, 50], we are convinced that the existence of two independent sets of binding sites has no physical meaning when dealing with interactions involving two macromolecules, in particular because of the simultaneous occurrence of several complex events as mentioned above. Hence, the use of the "2-stages structuring model" expression, underlying the presence of two distinct structuring phases instead of the "2-sites model" was more appropriate.

When using the "2-binding site model" as an approximation to extract the thermodynamic parameters of the interaction (namely, the affinity constant, Ka and binding reaction's enthalpy, ΔH) between LYS and PPI at the three experimental conditions, erroneous values with large errors were obtained (data not shown). Consequently, we were unable to quantify the binding parameters using the ITC Microcal associated origin software because the curves were complex and difficult to fit.

Although the appropriate thermodynamic parameters for the interaction between LYS and PPI could not be calculated, it was clear that the overall process leading to particle formation was enthalpically driven. A contrary situation occurred with the two other egg proteins tested, with no or only small negative heats detected by ITC. From the literature data [51, 52], enthalpy (ΔH) was related to the energy involved in molecular interactions and reflects the contribution of hydrogen bonds, electrostatic interactions, and van der Waals forces, while the change in entropy (T.ΔS) reflects a change in the order of the system and is related to hydrophobic interactions.

As possible particle formation between PPI and LYS was supposed from ITC data, the aqueous mixture of both proteins was further analyzed in terms of particle size, ζ-potential, and microstructure.
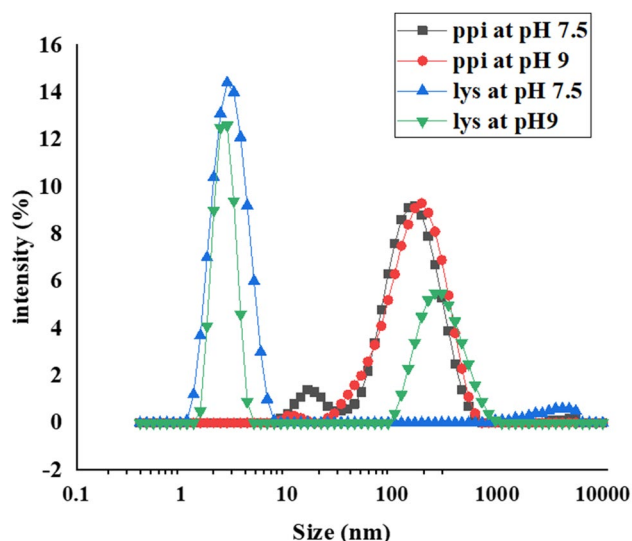

Fig. 3 Particle size distribution measured by DLS of PPI (0.008mM) and LYS (0.92 mM) suspensions in TRIS buffer at pH 7.5 and 9.0

LYS-PPI Aggregates Size Distribution

From the previous study of ITC, two steps in aggregation between PPI and LYS happened. To characterize the particle size of the solution of PPI and LYS, DLS was performed (Fig. 3).

Figure 3 showed that the size distribution of PPI evidenced a bimodal distribution at pH 7.5 and 9.0. Particles around 19 and 11 nm at pH 7.5 and 9, respectively, may correspond to 7 and 11 S oligomers, whereas those around 180 and 189 nm at pH 7.5 and 9.0, respectively, could be

Table 1 The D (4,3) values of LYS-PPI mixtures in TRIS buffer at pH 7.5 and 9.0

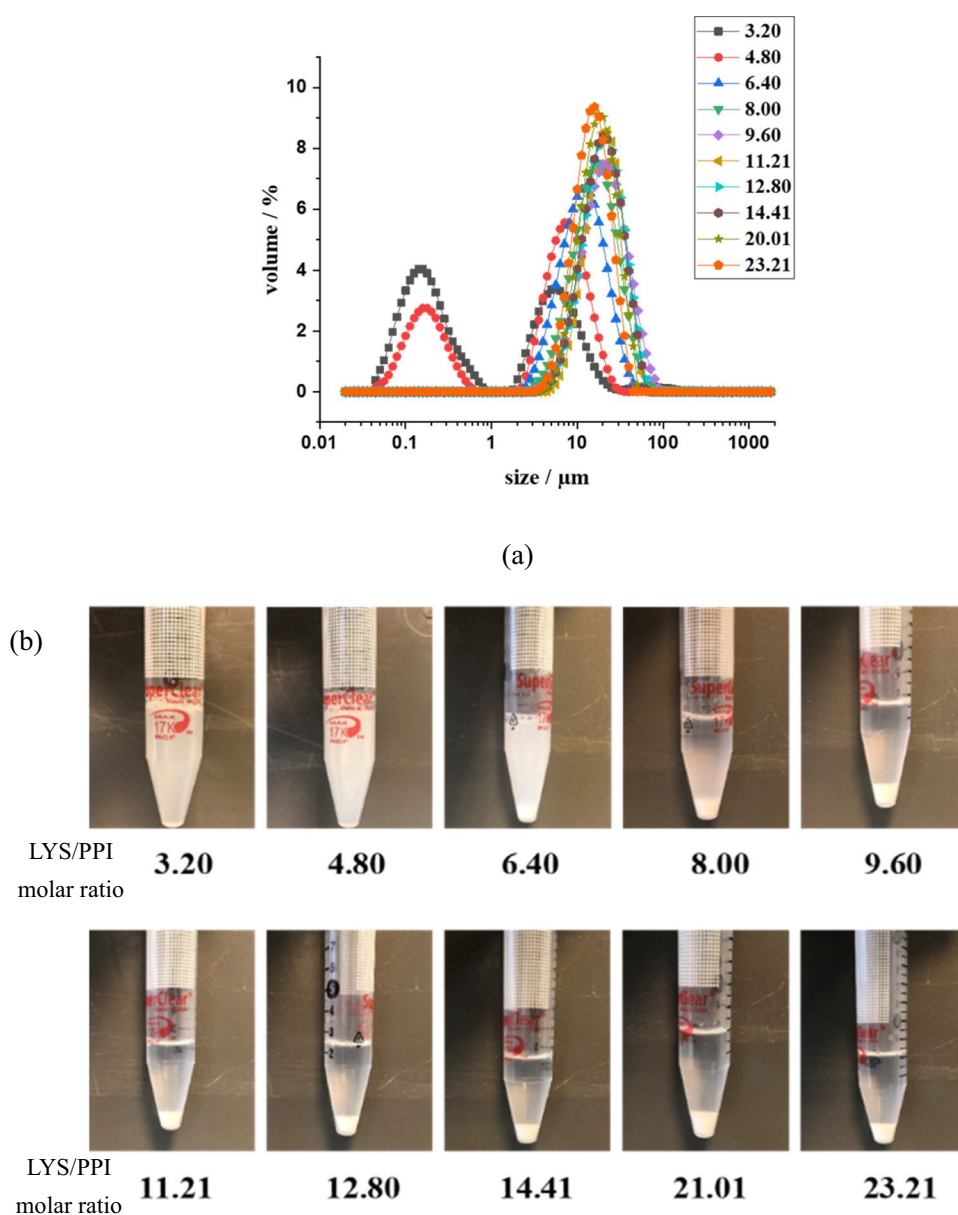| pH 7.5		pH 9.0	
Samples LYS/ PPI molar ratio	D [4,3] - Volume weighted mean (μm)	Samples LYS/ PPI molar ratio	D [4,3] - Volume weighted mean (μm)
3.2	5.2 ± 0.6a	5.2	4.9 ± 0.2a
4.8	6.2 ± 0.005a	8.7	5.5 ± 0.5a
6.4	12.8 ± 0.04b	12.2	11.8 ± 0.1b
8.0	21.7 ± 0.5de	14.0	21.9 ± 0.2c
9.6	22.7 ± 0.1df	15.7	27.2 ± 0.4e
11.2	25.3 ± 0.1 g	17.5	28.1 ± 0.2e
12.8	23.8 ± 0.2f	19.2	27.9 ± 0.2e
14.4	23.1 ± 0.2df	20.9	27.0 ± 0.5e
20.0	20.5 ± 0.1d	23.6	23.9 ± 0.2d
23.2	17.2 ± 0.1c	25.3	22.0 ± 0.2c

Means followed by different small letter for the same column are significantly different ($P < 0.05$)

aggregated protein particles formed during PPI preparation or initially present [36, 53]. The mean size of LYS at pH 7.5 and pH 9.0 was in the range of 2.5 to 3.0 nm, in line with the LYS monomer [54]. At pH 9.0, results also showed a double distribution where particles around 314 nm could originate from the aggregation of LYS resulting from less electrostatic repulsion between protein molecules at this pH closer to the Ip of LYS. To characterize aggregation for the mixture in a larger range of particle size, laser granulometry was used.

Figures 4 and 5 demonstrated the particle size distribution by laser granulometry (a) and visual appearance (b) of LYS-PPI mixtures at pH 7.5 and 9.0, respectively. The particle size of the mixtures formed by PPI and LYS at different LYS/PPI molar ratios were reported in Table 1 for the respective pH. As shown in Table 1, the size particle in the LYS-PPI mixture

at pH 7.5 showed two distinct situations. First, it increased with the increasing proportion of LYS, then decreased when the LYS/PPI molar ratio was more than 11.21. Table 1 also gave the mean particle size for the pH 9.0 counterparts, showing similar behavior to the results at pH 7.5 with a maximum particle size for a LYS/PPI molar ratio of 17.45. As the particle size decreased from a LYS/PPI molar ratio of ~11 at pH 7.5 and 17 at pH 9.0, respectively (Table 1), it could be hypothesized that mixed aggregates became more and more compact from this threshold, as repulsive forces between aggregates increased with the addition of LYS. This increased the density of the aggregates which led to increase their precipitation, as suggested by the lower quantity of the protein material on the CLSM pictures (Fig. 7g and h). Furthermore, Figs. 4b and 5b showed the visual appearance of

Fig. 4 Particle size distribution by laser granulometry (**a**) and pictures (**b**) of LYS-PPI suspensions at different LYS/PPI molar ratio in TRIS buffer pH 7.5
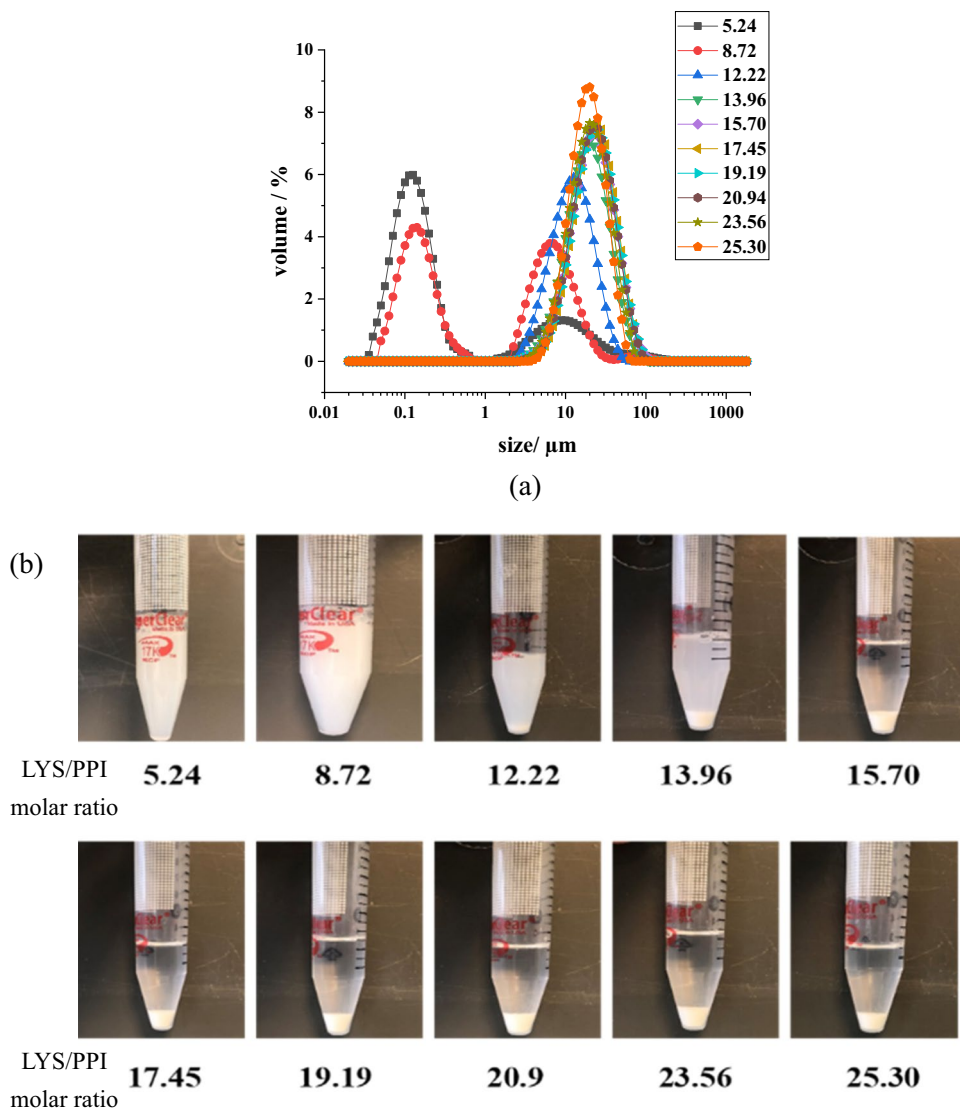

(a)

(b)

LYS-PPI mixtures at different molar ratios at pH 7.5 and 9.0, respectively. Precipitates were observed directly after mixing PPI and LYS as the molar ratio exceeded the inflection point previously revealed for ITC binding isotherms, i.e. > 5 and > 12 at pH 7.5 and 9.0 respectively.

Relationship Between Protein Charge and Aggregates Size

The ζ-Potential of PPI, LYS, and their mixtures were measured in TRIS buffer at pH 7.5 and 9.0 (Fig. 6a-b). The ζ-Potential of PPI and LYS as a function of pH was also presented in Fig. 6c. The points where ζ-Potential change from positive to negative values indicated the Ip of PPI and LYS were around 4.9 and 10.7, respectively, in good agreement with the previously reported Ip values of these proteins [55–58]. Therefore, LYS showed a positive charge at pH 7.5 and 9.0, whereas PPI showed a negative charge respectively.

At both pHs, the LYS-PPI mixture's charge increases with LYS content, ranging from a negative charge at the smaller LYS/PPI ratio in the mixture to a positive charge at a higher LYS ratio in the mixture. The variation of the ζ-Potential showed a typical charge inversion from positive ζ-Potential values when the polycation was in excess to negative ones when the polyanion was in excess (Fig. 6) in line with the recent work of Rodriguez et al. [59]. We can hypothesize that positive charges of LYS interacted with negatively charged segments of PPI, leading to the formation of electrostatic complexes. This behavior indicated the presence of interactions between the carboxyl groups of PPI and the amino group of LYS, featuring electrostatic binding. The charge was null for molar ratios close to 12 and 21 at pH 7.5 and 9.0, respectively. These results agreed with the previous results of ITC where the enthalpy didn't change anymore with the increasing proportion of LYS from similar molar ratios (Fig. 2). It could indicate that at these concentrations, LYS molecules had completely counteracted PPI charges.

Fig. 5 Particle size distribution by laser granulometry (**a**) and pictures (**b**) of LYS-PPI suspensions at different LYS/PPI molar ratios in TRIS buffer at pH 9.0

(a)

(b)

Confocal Microscopic Observations of Aggregates

In order to better understand the microstructural properties and aggregation phenomena in LYS-PPI mixture systems, PPI and LYS stock solution and six suspensions at different LYS/PPI molar ratios (0.8, 1.6, 3.2, 4.8, 11.2, and 20) were analyzed by CLSM at pH 7.5 (Fig. 7). The white color indicated the protein particles stained by Fast Green.

From Fig. 7a, the PPI solution showed homogeneous distribution of tiny particles. A similar microstructure was previously reported for soluble PPI [60]. LYS showed aggregates (Fig. 7b) that may be due to some impurities in LYS powder introduced during purification or drying and/or to traces of misfolded lysozyme, as suggested by Nikarjam et al. [61]. However, when mixed with the PPI solution, the aggregates dissociated with dilution and no more aggregates were observed as suggested by DLS results (Fig. 3). As the concentration of LYS increased, large aggregates with increased size were observed (Fig. 7c to h), in agreement with the previous particle size results (Fig. 5). These protein aggregates had heterogeneous forms with irregular shapes. This increased size of protein particles could be attributed to strong attractive interactions between the two oppositely charged proteins (i.e., PPI and LYS) and contributed to form larger aggregated complexes which increased with LYS addition. As the particle size decreased from a LYS/PPI molar ratio of ~ 11 at pH 7.5 (Table 1), it could be hypothesized that mixed aggregates became more and more compact and more and more individualized from this threshold. Similar CLSM images of complex aggregation were also previously reported in PPI-low-methoxyl pectin mixture [60], whey protein–beet pectin [62], and soybean protein-chitosan [63]. Obviously, the present results showed that no spherical-shaped aggregates between PPI and LYS were formed excluding the possibility of complex coacervation in the studied conditions.

Conclusion

The interactions and aggregation phenomena of pea proteins with three different egg white proteins were investigated. Only weak interaction was detected between PPI and acidic or neutral proteins from egg like OVA and OVT, respectively. Special attention was paid to the mixture of PPI and LYS which showed specific interaction–aggregation behavior. It was evidenced that non-spherical aggregates were formed from low LYS/PPI molar ratio growing into large irregular aggregated structures that insolubilized at high molar ratio excluding the formation of pure complex coacervates. By combining the results obtained by the different techniques implemented here, we proposed a simple mechanism for the interaction–aggregation that occured when LYS was mixed with PPI. At low ionic strength, LYS

interacted with PPI at pH 7.5 and pH 9.0 according to two major structuring step processes: (i) the first step led to the spontaneous formation of soluble complexes, and (ii) the second step involved the aggregation of these structures to
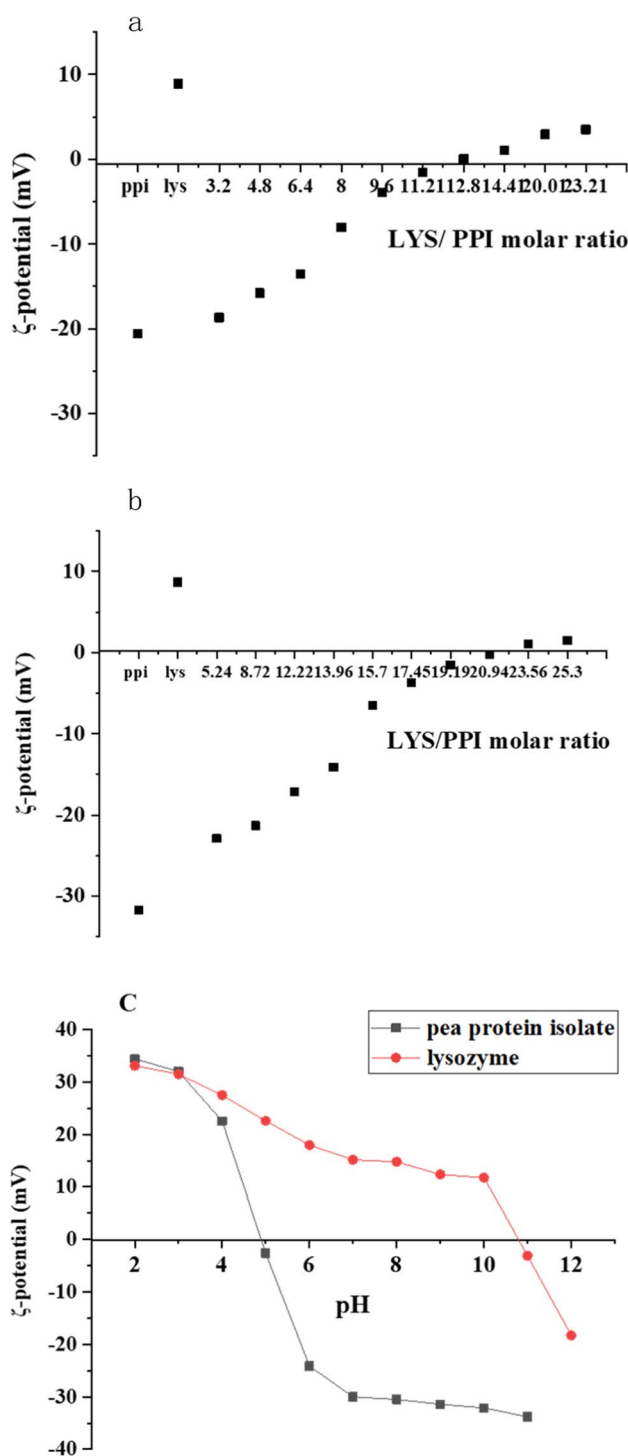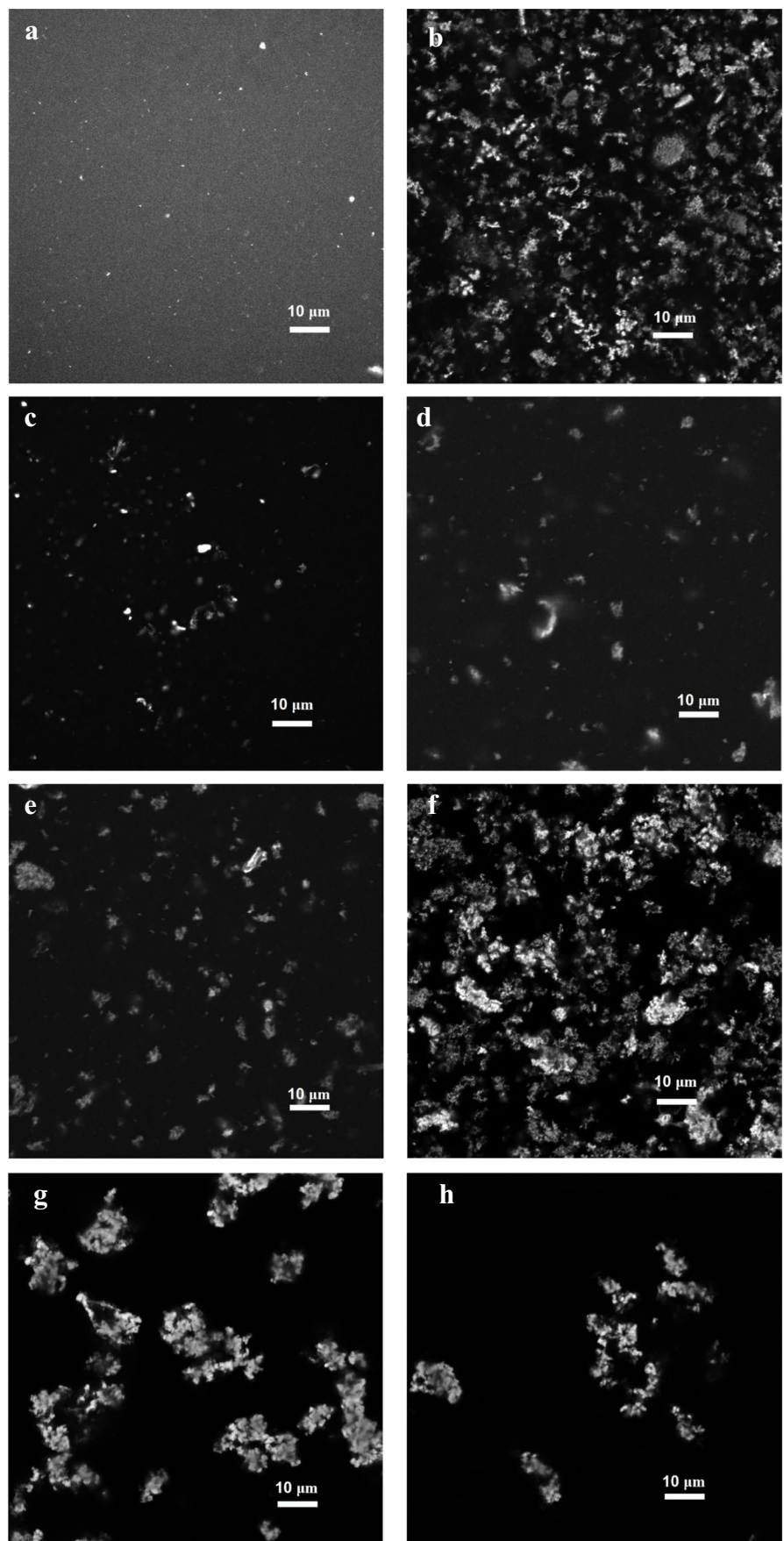

Fig. 6 The ζ-potential of LYS-PPI mixtures as a function of LYS/PPI molar ratios in TRIS buffer at pH 7.5 (**a**) and pH 9.0 (**b**), and of PPI and LYS solutions as a function of pH (**c**)

Fig. 7 Microscopic observations by CLSM of mixed LYS-PPI suspensions at 20 °C in TRIS buffer at pH 7.5: PPI (**a**), LYS (**b**), and LYS/PPI molar ratio of 0.8 (**c**), 1.6 (**d**), 3.2 (**e**), 4.8 (**f**), 11.2 (**g**), 20 (**h**)

form large separated aggregates with higher size centered around 20–25 μm. The transition from step 1 to step 2 was governed by pH-dependent protein stoichiometry needed to achieve opposite charge compensation. This transition occured at a lower LYS/PPI ratio at pH 7.5 thanks to the higher surface positive charge of LYS as compared to pH 9.0. These results suggested that LYS, as egg basic protein, will play a key interacting role when PPI is mixed with egg white for application purpose that deserves to be studied in depth in such a complex system.

Declarations

Competing Interests The authors declare no competing interests.

Conflict of Interest The authors declare no competing interests.

References

1. M. Henchion, M. Hayes, A.M. Mullen, M. Fenelon, B. Tiwan, Foods **6**(7), 53 (2017)
2. FAO. Notes on livestock, food security and gender equity. Animal Production and Health Working Paper. No. 3. Rome, Italy (2011)
3. United Nations General Assembly. Resolution adopted by the general assembly on 25 September 2015. A/RES/70/1 Transforming Our World: the 2030 Agenda for Sustainable Development (2015)
4. A.C. Alves, G.M. Tavares, Food Hydrocoll. **97**, 105171 (2019)
5. J. Davis, U. Sonesson, D.U. Baumgarten, T. Nemecek, Food Res. Int. **43**(7), 1874–1884 (2010)
6. J. Boye, F. Zare, A. Pletch, Food Res. Int. **43**(2), 414–431 (2010)
7. S.R. Hertzler, J.C. Lieblein-Boff, M. Weiler, C. Allgeier, Nutrients **12**(12), 3704 (2020)
8. I. Ersch, E. ter Laak, P. van der Linden, A. Venema, Martin, Food Hydrocoll. **44**, 59–65 (2015)
9. W.N. Ainis, C. Ersch, R. Ipsen, Food Hydrocoll. **77**, 397 (2017)
10. E.B. Hinderink, L. Sagis, K. Schroën, C.C. Berton-Carabin, Coll. Surf. B: Biointerfaces **192**, 111015 (2020)
11. F. Guyomarc'h, G. Arvisenet, S. Bouhallab, F. Canon, S.-M. Deutsch, V. Drigon, D. Dupont, M.-H. Famelart, G. Garric, E. Guédon, T. Guyot, M. Hiolle, G. Jan, Y. Le Loir, V. Lechevalier, F. Nau, S. Pezennec, A. Thierry, F. Valence, V. Gagnaire, Trends Food Sci. Technol. **108**, 119–132 (2021)
12. H.C.J. Godfray, P. Aveyard, T. Garnett, J.W. Hall, T.J. Key, J. Lorimer, R.T. Pierrehumbert, P. Scarborough, M. Springmann, S.A. Jebb, Science **361**, eaam5324 (2018)
13. R.W. Burley, D.V. Vadehra (eds.), John Wiley & Sons, New York, p 65 (1989)
14. H.D. Belitz, W. Grosch, P. Schieberle, *Food Chemistry: 4th Reversed and Extended Edition*. (Springer, Heidelberg, 2009), pp. 546–562
15. P. Shih, J.F. Kirsch, Protein Sci. **4**(10), 2063–2072 (1995)
16. P. Shih, D.R. Holland, J.F. Kirsch, Protein Sci. **4**(10), 2050–2062 (1995)
17. T. Ueda, K. Masumoto, R. Ishibashi, T. So, T. Imoto, Protein Eng. **13**(3), 193–196 (2000)
18. Y. Su, Y. Dong, F. Niu, C. Wang, Y. Liu, Y. Yang, Y Eur. Food Res. Technol. **240**(2), 367–378 (2015)
19. T. Zhang, J. Guo, J.F. Chen, J.M. Wang, Z.L. Wan, X.Q. Yang, Food Hydro. **100**, 105449 (2020)
20. F. Alavi, Z. Emam-Djomeh, L. Chen, Food Hydro. **107**, 105960 (2020)
21. J. Zheng, C.H. Tang, G. Ge, M. Zhao, W. Sun, Food Hydro. **101**, 105571 (2020)
22. F.E. O'Kane, R.P. Happe, J.M. Vereijken, H. Gruppen, M.A. van Boekel, J. Agric. Food Chem. **52**(16), 5071–5078 (2004)
23. C.D. Munialo, A.H. Martin, E. Van Der Linden, H.H. De Jongh, J. Agric. Food Chem. **62**(11), 2418–2427 (2014)
24. T.G. Burger, Y. Zhang, Trends Food Sci. Technol. **86**, 25–33 (2019)
25. R.E. Aluko, O.A. Mofolasayo, B.M. Watts, J. Agric. Food Chem. **57**(20), 9793–9800 (2009)
26. H.N. Liang, C.H. Tang, Food Hydro. **33**(2), 309–319 (2013)
27. A.P. Adebiyi, R.E. Aluko, Food Chem. **128**, 902 (2011)
28. J. Gueguen, Plant. Foods Hum. Nutr. **32**(3), 267–303 (1983)
29. J.A. Gatehouse, R.R.D. Croy, H. Morton, M. Tyler, D. Boulter, Eur. J. BioChem. **118**(3), 627–633 (1981)
30. F.E. O'Kane, R.P. Happe, J.M. Vereijken, H. Gruppen, M.A. van Boekel, J. Agric. Food Chem. **52**(10), 3141–3148 (2004)
31. J.-L. Mession, S. Roustel, R. Saurel, Food Hydrocoll. **67**(Supplement C), 229–242 (2017)
32. H.T. Kristensen, A.H. Møller, M. Christensen, M.S. Hansen, M. Hammershøj, T.K. Dalsgaard, Int. J. Food Sci. Technol. **55**(8), 2920–2930 (2020)
33. H.T. Kristensen, Q. Denon, I. Tavernier, S.B. Gregersen, M. Hammershøj, P. Van Der Meeren, … T. K. Dalsgaard. Food Hydro. **113**, 106556 (2021)
34. H.T. Kristensen, M. Christensen, M.S. Hansen, M. Hammershøj, T.K. Dalsgaard, Int. J. Food Sci. Technol. **56**(11), 5777–5790 (2021)
35. H.T. Kristensen, M. Christensen, M.S. Hansen, M. Hammershøj, T.K. Dalsgaard, Food Chem. **373**, 131509 (2022)
36. M.L. Chihi, J.L. Mession, N. Sok, R. Saurel, J. Agric. Food Chem. **64**(13), 2780–2791 (2016)
37. T. Croguennec, F. Nau, S. Pezennec, G. Brule, J. Agric. Food Chem. **48**(10), 4883–4889 (2000)
38. A.O.A.C. Official methods of Analysis: 15th edition. Ed by Association of Official Analytical Chemists, Washington DC (1990)
39. J. Mosse, J. Agric. Food Chem. **38**(1), 18–24 (1990)
40. H. Greenfield, D.A.T. Southgate, Rome: Food and Agriculture Organization of the United Nations, 2nd edn. (2007)
41. A. Halabi, T. Croguennec, O. Ménard, V. Briard-Bion, J. Jardin, Y. Le Gouar, A. Deglaire, Food Hydrocoll. **126**, 107368 (2022)
42. G. Somaratne, F. Nau, M.J. Ferrua, J. Singh, A. Ye, D. Dupont, J. Floury, Food Hydrocoll. **98**, 105228 (2020)
43. M. Rabiller-Baudry, B. Chaufer, J. Chromatogr. B: Biomed. Sci. Appl. **753**(1), 67–77 (2001)
44. M. Nigen, V. Le Tilly, T. Croguennec, D. Drouin-Kucma, S. Bouhallab, Biochim. Biophys. Acta (BBA)-Proteins Proteomics **1794**(4), 709–715 (2009)
45. M. Nigen, T. Croguennec, D. Renard, S. Bouhallab, BioChem. **46**(5), 1248–1255 (2007)

46. J. Zheng, Q. Gao, G. Ge, J. Wu, C.H. Tang, M. Zhao, W. Sun, Food Hydrocoll. **124**, 107247 (2022)

47. T. Croguennec, G.M. Tavares, S. Bouhallab, Adv. Coll. Interface Sci. **239**, 115–126 (2017)

48. M.L. Doyle, P. Hensley, In Proteomics and Protein-Protein Interactions (pp. 147–163). Springer, Boston, MA. (2005). https://doi.org/10.1007/0-387-24532-4_7

49. M. Girard, S.L. Turgeon, S.F. Gauthier, J. Agric. Food Chem. **51**(15), 4450–4455 (2003)

50. L. Aberkane, J. Jasniewski, C. Gaiani, J. Scher, C. Sanchez, Langmuir **26**(15), 12523 (2010)

51. S. Leavitt, E. Freire, Curr. Opin. Struct. Biol. **11**(5), 560–566 (2001)

52. G. Klebe, Nat. Rev. Drug Discov. **14**(2), 95–110 (2015)

53. X. Li, Y. Li, Y. Hua, A. Qiu, C. Yang, S. Cui, Food Chem. **104**(4), 1410–1417 (2007)

54. J. Zheng, Q. Gao, G. Ge, J. Wu, C.H. Tang, M. Zhao, W.J. Sun, Agric. Food Chem **69**(28), 7948 (2021)

55. K. Rezwan, A.R. Studart, J. Vörös, L.J. Gauckler, J. Phys. Chem. B **109**(30), 14469–14474 (2005)

56. D.R. Klassen, M.T. Nickerson, Food Res. Int **46**(1), 167–176 (2012)

57. I. Yadav, S. Kumar, V.K. Aswal, J. Kohlbrecher, Langmuir **33**(5), 1227–1238 (2017)

58. H. Helmick, C. Hartanto, A. Bhunia, A. Liceaga, J.L. Kokini, Food Biophys. **16**(4), 474–483 (2021)

59. A.M.B. Rodriguez, B.P. Binks, T. Sekine, Soft Matter **14**(2), 239–254 (2018)

60. Y. Lan, J.B. Ohm, B. Chen, J. Rao, Food Hydrocoll. **101**, 105556 (2020)

61. S. Nikfarjam, M. Ghorbani, S. Adhikari, A.J. Karlsson, E.V. Jouravleva, T.J. Woehl, M.A. Anisimov, Colloid J. **81**, 546–554 (2019)

62. B. Chen, H. Li, Y. Ding, H. Suo, LWT-Food Sci. Technol. **47**(1), 31–38 (2012)

63. Y. Yuan, Z.L. Wan, X.Q. Yang, S.W. Yin, Food Res. Int. **55**, 207–214 (2014)